Journal of Stress Analysis
Vol. 5, No. 1, Spring − Summer 2020, 121-134

Bu-Ali Sina University

ORIGINAL RESEARCH PAPER

Analytical Solution of the Coupled Dynamic Thermoelasticity Problem in a Hollow Cylinder

H. Sharifi Torki, A.R. Shahani*

Mechanical Engineering Department, K.N. Toosi University of Technology, Tehran, Iran.

Article info

Article history:
Received 22 June 2020
Received in revised form
12 September 2020
Accepted 19 September 2020

Keywords:
Thermoelasticity
Coupled
Thick-walled cylinder
Transient loading
Hankel transform

Abstract

The fully classical coupled thermoelasticity problem in a thick hollow cylinder is solved using analytical methods. Finite Hankel transform, Laplace transform and a contemporary innovative method are used to solve the problem and presenting closed-form relations for temperature and stress distribution. To solve the energy equation and the structural equation, on the inner and the outer surfaces of the cylinder, time-dependent thermal and mechanical boundary conditions are applied. The Dirichlet boundary condition which represents temperature, is considered to solve the energy equation and the Cauchy boundary condition which represents traction, is considered for the equation of motion. Two cases are studied numerically, pure mechanical load and pure thermal load. In plotting the results for the case of prescribing pure mechanical load in spite of not applying any thermal load induced temperature can be seen in the temperature history figure. Due to solving the elastodynamic problem, the elastic and the thermoelastic stress wave propagation into the medium and the reflection were observed in the plotted results.

Nomenclature

a	Inner radius	b	Outer radius
c	Specific heat	α	Thermal expansion coefficient
k	Thermal conductivity	ρ	Density
E	Modulus of elasticity	v	Poisson's ratio
θ	Temperature	u	Displacement
t	Time	T_0	Reference temperature
σ_{rr}	Radial stress	$\sigma_{\theta\theta}$	Hoop stress
H	Hankel transform	P	Applied pressure on the inner surface
t^*	Time of reaching dilatation wave to a specific radial position	V_e	Velocity of the wave
		θ_0	Applied temperature on the inner surface

1. Introduction

A large number of mechanical elements are affected by thermal loads and in some cases these loads are large enough to cause structural failure. Due to this widespread applications, classical and generalized theories of thermoelasticity are developed. The equations of thermoelasticity are coupled, i.e., a change

*Corresponding author: A.R. Shahani (Professor)
E-mail address: shahani@kntu.ac.ir
http://dx.doi.org/10.22084/jrstan.2020.22464.1155
ISSN: 2588-2597

in the temperature field produces a strain and mutually time-dependent deformation leads to the change in the temperature field. The equations of the coupled classical thermoelasticity theory are very complicated due to thermo-mechanical coupling terms that exist between displacement and temperature components. Therefore structural equation and energy equation must be solved simultaneously. Due to this complexity, analytical solutions have not been extended widely. Analytical solution of quasi-static and dynamic uncoupled thermoelasticity problem in a thick sphere presented by Shahani and Momeni Bashusqeh [1] in 2014. They [2] also solved the coupled classical thermoelasticity problem in a thick sphere in 2013. Shahani and Nabavi [3] solved quasi-static classical thermoelasticity problem in a thick hollow cylinder. They used finite Hankel transform to solve the energy equation. Thermal boundary conditions are considered to be time-dependent and two different cases of mechanical boundary conditions are investigated. They also established one to one relations between tractions and displacement on the boundaries. Yun et al. [4] obtained thermal stress distribution in a thick cylinder subjected to thermal shock. They used Dirac function to model boundary condition of thermal shock and Laplace transform to solve uncoupled heat conduction equation. The problem is considered to be quasi-static.

Raoofian Naeeni et al. [5] presented analytical solution for coupled thermoelastic transient waves in a half-space made of transversely isotropic material. They used a new potential function to uncouple the equation of motion and the heat conduction equation and then solved the problem using Hankel and Laplace transforms. Liang et al. [6] proposed an asymptotic method for solving transient thermal shock in isotropic medium with temperature dependent properties. They solved the system of equations using integral transform method. A sudden temperature rise is applied as boundary condition.

Wang [7] studied hollow cylinder which is subjected to rapid arbitrary heating. A uniform temperature is considered in the entire hollow cylinder which makes the problem uncoupled. The finite Hankel transform is used to obtain displacement field. Cho et al. [8] used Hankel transform and Laplace transform to obtain dynamic thermal stress distribution in a thick-walled orthotropic cylinder. The energy equation is not solved and a constant temperature distribution is considered to obtain stress components. Ding et al. [9] solved dynamic plane strain thermoelasticity problem for a non-homogeneous orthotropic cylindrical shell using the orthogonal expansion technique. Zhou et al. [10] studied dynamic thermal stresses in a short thick-walled orthotropic tube based on high order shell theory. Cubic and quadratic forms are considered for axial and radial displacements and the equation of motion is solved using precise integration method.

Vel [11] used power series technique to present a solution for three-dimensional thermoelasticity problem of a functionally graded long hollow cylinder. The material properties are considered to be cylindrically monoclinic and temperature dependent. An axial force and torque are applied on the cylinder as well as prescribing loads on the surfaces.

Marin [12] developed the domain of influence theorem to investigate the thermoelasticity of bodies with voids. In this work it is proved that for a finite time, temperature and displacement fields do not create disturbance outside the bounded domain. Rychahivskyy and Tokovyy [13] used direct integration method to solve elasticity and thermoelasticity equations in a semi-plane for different types of boundary conditions.

Shahani and Sharifi Torki [14] solved dynamic classical thermoelasticity problem in an isotropic thick hollow cylinder. The strain rate term in the heat conduction equation is ignored to make the equations of thermoelasticity uncoupled. The inner and the outer surfaces of the cylinder are subjected to time-dependent thermal and mechanical loadings. They also [15] studied thermoelastic wave propagation in an orthotropic thick hollow cylinder. They used classical uncoupled theory of thermoelasticity and considered the problem to be dynamic. An exponentially decaying temperature is prescribed on the inner surface and then propagation and reflection of thermal stress wave are studied for two different types of mechanical boundary conditions. Tarn [16] presented exact solutions for temperature distribution, thermal stresses and deformations in an anisotropic hollow and solid cylinders. The uncoupled theory of thermoelasticity is used and the material properties are considered to be radial dependent.

Itu et al. [17] proposed a mathematical model to increase the stiffness of composite plates. They used finite element method to perform static and modal analysis and verified the results by the experimental tests. Lata and Kaur [18] studied deformation of a homogeneous transversely isotropic circular plate subjected to thermomechanical loadings. The lateral surfaces of the plate are considered to be traction free. They also investigated the effects of two temperature thermoelasticity on the deformation of the plate.

Valse et al. [19] presented a theoretical background to study dynamic of multi body systems using finite element methods. They used Lagrange's equations and considered the one-dimensional elastic elements to analyze the problem of general three-dimensional motion.

Mishra et al. [20] presented closed-form solution for the forced vibration of non-homogenous isotropic thin annular disk subjected to dynamic pressure. Lord-Shulman theory and Laplace transform are used to solve the problem. Thermal and mechanical properties of the material vary according to power law distribution in radial coordinate. Sharma et al. [21] derived the relations and equations for non-local thermoelastic solid with diffusion. They also studied the free vibration of diffusive hollow cylinder using generalized theory of thermoelasticity. To transform the governing equations to ordinary differential equations the vibration of the cylinder is considered to be time harmonic. Abbas [22] used eigenvalue method to obtain analytical solution for free vibration of thermoelastic hollow sphere. For the mechanical boundary conditions both the inner and the outer surfaces of the sphere are considered to be stress free. A constant temperature is applied as thermal boundary condition and generalized theory of thermoelasticity with one relaxation time is used to solve the problem.

In this paper fully coupled classical thermoelasticity problem in a thick hollow cylinder is solved analytically using transformation methods and closed-form relations are presented for the temperature field and the distribution of the stress components. An outstanding difference between this work and previous papers such as [14] and [15] is the use of coupled theory of thermoelasticity. To show the effect of the thermo-mechanical coupling, two different load cases are investigated; pure mechanical load and pure thermal load. In the pure mechanical load case an induced temperature gradient can be seen in the figures which is the direct impact of the coupling term. Existence of this thermo-mechanical coupling, the strain rate term in the energy equation, increases the precision of the results but makes the problem complicated and the thermoelasticity equations should be solved concurrently. To validate the presented solution and the results, the problem of a hollow cylinder subjected to the uniform and constant temperature distribution is solved and the results are compared with those presented by Ding et al. [9] which shows good agreement.

2. Formulation

Consider a long hollow circular cylinder made of homogeneous isotropic material with inner and outer radii a and b, respectively. The geometry is shown in Fig. 1.

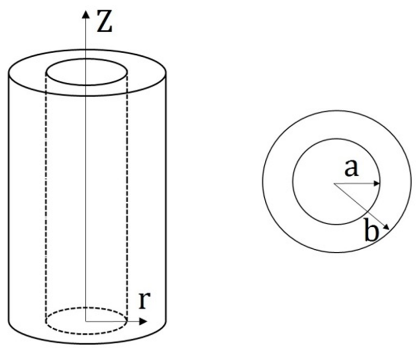

Fig. 1. Schematic geometry of the problem.

Due to symmetry, the equations of the coupled thermoelasticity in cylindrical coordinates reduce to [23]:

$$\frac{\partial^2\theta}{\partial r^2}+\frac{1}{r}\frac{\partial\theta}{\partial r}-\frac{1}{\alpha^*}\frac{\partial\theta}{\partial t}=\frac{E\alpha T_0}{k(1-2v)}\left(\frac{\partial\dot{u}}{\partial r}+\frac{\dot{u}}{r}\right) \tag{1a}$$

$$\frac{\partial^2 u}{\partial r^2}+\frac{1}{r}\frac{\partial u}{\partial r}-\frac{1}{r^2}u-\gamma^2\ddot{u}=\beta\frac{\partial\theta}{\partial r} \tag{1b}$$

where:

$$\gamma^2=\frac{\rho}{E}\frac{(1+v)(1-2v)}{(1-v)} \tag{2a}$$

$$\beta=\alpha\frac{(1+v)}{(1-v)} \tag{2b}$$

$$\alpha^*=\frac{k}{\rho c} \tag{2c}$$

in which ρ, v and E are the density, the Poisson's ratio the modulus of elasticity respectively. Also α is the thermal expansion coefficient, k coefficient of the thermal conduction and c the specific heat. On the other hand, we have:

$$\theta=T(r,t)-T_0 \tag{3a}$$

$$u=u(r,t) \tag{3b}$$

where T_0 is the reference temperature at which the cylinder is stress free. The right-hand side of Eq. (1a) which is the strain rate, is the thermo-mechanical coupling term. This term and the right-hand side of Eq. (1b) cause the reciprocal interactions of temperature and displacement fields. The stress components are σ_{rr} and $\sigma_{\theta\theta}$ which include mechanical and thermal parts [23]:

$$\sigma_{rr}=\frac{E}{(1+v)(1-2v)}\left[(1-v)\frac{\partial u}{\partial r}+v\frac{u}{r}\right]-\frac{E\alpha}{(1-2v)}\theta \tag{4a}$$

$$\sigma_{\theta\theta}=\frac{E}{(1+v)(1-2v)}\left[v\frac{\partial u}{\partial r}+(1-v)\frac{u}{r}\right]-\frac{E\alpha}{(1-2v)}\theta \tag{4b}$$

On the inner and the outer surfaces of the cylinder thermal boundary conditions are applied as follows:

$$\theta(a,t)=f(t) \tag{5a}$$

$$\theta(b,t)=g(t) \tag{5b}$$

where $f(t)$ and $g(t)$ are known time-dependent functions. The initial condition temperature of the cylinder is considered to be radial dependent:

$$\theta(r,0)=F_1(r) \tag{6}$$

Time-dependent traction boundary conditions are applied on the inner and the outer surfaces of the cylinder:

$$\sigma_{rr}(a,t) = P_1(t) \tag{7a}$$

$$\sigma_{rr}(b,t) = P_2(t) \tag{7b}$$

By substituting (7a) and (7b) in (4a) we have:

$$\left.\frac{\partial u}{\partial r}\right|_{r=a} + h_1 u(a,t) = B_1(t) \tag{8a}$$

$$\left.\frac{\partial u}{\partial r}\right|_{r=b} + h_2 u(b,t) = B_2(t) \tag{8b}$$

where:

$$h_1 = \frac{v}{(1-v)a} \tag{9a}$$

$$h_2 = \frac{v}{(1-v)b} \tag{9b}$$

$$B_1(t) = -\frac{(1+v)(1-2v)}{E(1-v)}P_1(t) + \frac{(1+v)\alpha}{(1-v)}f(t) \tag{9c}$$

$$B_2(t) = -\frac{(1+v)(1-2v)}{E(1-v)}P_2(t) + \frac{(1+v)\alpha}{(1-v)}g(t) \tag{9d}$$

The initial conditions for the structural equation are:

$$u(r,0) = F_2(r) \tag{10a}$$

$$\dot{u}(r,0) = F_3(r) \tag{10b}$$

where $F_2(r)$ and $F_3(r)$ are known radial dependent functions and a dot over the quantity is the partial derivative of the function with respect to time.

3. The Method of Solution

To solve the coupled thermoelasticity equations $\theta(r,t)$ and $u(r,t)$ are resolved into two parts:

$$u(r,t) = u_1(r,t) + u_2(r,t) \tag{11a}$$

$$\theta(r,t) = \theta_1(r,t) + \theta_2(r,t) \tag{11b}$$

Applying Eq. (11b) to Eq. (1a) and its boundary and initial conditions, Eq. (5) and Eq. (6), results in separating the heat conduction equation into two boundary value problems:

$$\frac{\partial^2\theta_1}{\partial r^2} + \frac{1}{r}\frac{\partial\theta_1}{\partial r} - \frac{1}{\alpha^*}\frac{\partial\theta_1}{\partial t} = 0 \tag{12a}$$

$$\theta_1(a,t) = f(t) \tag{12b}$$

$$\theta_1(b,t) = g(t) \tag{12c}$$

$$\theta_1(r,0) = 0 \tag{12d}$$

and

$$\frac{\partial^2\theta_2}{\partial r^2} + \frac{1}{r}\frac{\partial\theta_2}{\partial r} - \frac{1}{\alpha^*}\frac{\partial\theta_2}{\partial t} = \frac{E\alpha T_0}{k(1-2v)}\left(\frac{\partial\dot{u}}{\partial r} + \frac{\dot{u}}{r}\right) \tag{13a}$$

$$\theta_2(a,t) = f(t) \tag{13b}$$

$$\theta_2(b,t) = g(t) \tag{13c}$$

$$\theta_2(r,0) = 0 \tag{13d}$$

In the same way by applying the Eq. (11a) to Eqs. (1b), (8) and (10), the structural problem can be resolved into the following equations:

$$\frac{\partial^2 u_1}{\partial r^2} + \frac{1}{r}\frac{\partial u_1}{\partial r} - \frac{1}{r^2}u_1 - \gamma^2\ddot{u}_1 = 0 \tag{14a}$$

$$\left.\frac{\partial u_1}{\partial r}\right|_{r=a} + h_1 u_1(a,t) = B_1(t) \tag{14b}$$

$$\left.\frac{\partial u_1}{\partial r}\right|_{r=b} + h_2 u_1(b,t) = B_2(t) \tag{14c}$$

$$u_1(r,0) = 0 \tag{14d}$$

$$\dot{u}_1(r,0) = 0 \tag{14e}$$

and

$$\frac{\partial^2 u_2}{\partial r^2} + \frac{1}{r}\frac{\partial u_2}{\partial r} - \frac{1}{r^2}u_2 - \gamma^2\ddot{u}_2 = \beta\frac{\partial\theta}{\partial r} \tag{15a}$$

$$\left.\frac{\partial u_2}{\partial r}\right|_{r=a} + h_1 u_2(a,t) = 0 \tag{15b}$$

$$\left.\frac{\partial u_2}{\partial r}\right|_{r=b} + h_2 u_2(b,t) = 0 \tag{15c}$$

$$u_2(r,0) = F_2(r) \tag{15d}$$

$$\dot{u}_2(r,0) = F_3(r) \tag{15e}$$

The solutions of Eqs. (12) and (14) can be accomplished applying the finite Hankel transform defined as [24]:

$$H[\theta_1(r,t);\zeta_n] = \bar{\theta}_1(\zeta_n,t) = \int_a^b r\theta_1(r,t)K_1(\zeta_n,r)dr \tag{16a}$$

$$H[u_1(r,t);\xi_m] = \bar{u}_1(\xi_m,t) = \int_a^b r u_1(r,t)K_2(\xi_m,r)dr \tag{16b}$$

where $K_1(\zeta_n,r)$ and $K_2(\xi_m,r)$ are the kernels of the transformation. Choosing the appropriate kernel for transformation is dependent on the equations and the related boundary conditions. The kernels of transformations for the present problem are as follows [25]:

$$K_1(r,\zeta_n) = J_0(\zeta_n r)Y_0(\zeta_n a) - J_0(\zeta_n a)Y_0(\zeta_n r) \quad (17a)$$

$$K_2(r,\xi_m) = \{J_1(\xi_m r)[\xi_m Y_1'(\xi_m a) + h_1 Y_1(\xi_m a)] - Y_1(\xi_m r)[\xi_m J_1'(\xi_m a) + h_1 J_1(\xi_m a)]\}1 \quad (17b)$$

where ζ_n and ξ_m are the positive roots of the following characteristics equations:

$$J_0(\zeta_n b)Y_0(\zeta_n a) - J_0(\zeta_n a)Y_0(\zeta_n b) = 0 \quad (18a)$$

$$[\xi_m Y_1'(\xi_m a + h_1 Y_1(\xi_m a)][\xi_m J_1'(\xi_m b) + h_2 J_1(\xi_m b)] - [\xi_m Y_1'(\xi_m b) + h_2 Y_1(\xi_m b)] \times [\xi_m J_1'(\xi_m a) + h_1 J_1(\xi_m a)] = 0 \quad (18b)$$

The inverse transforms are defined as [25]:

$$H^{-1}[\bar{\theta}_1(\zeta_n,t);r] = \theta_1(r,t) = \sum_{n=1}^{\infty} a_n \bar{\theta}_1(\zeta_n,t)K_1(r,\zeta_n) \quad (19a)$$

$$H^{-1}[\bar{u}_1(\xi_m,t);r] = u_1(r,t) = \sum_{m=1}^{\infty} b_m \bar{u}_1(\xi_m,t)K_2(r,\xi_m) \quad (19b)$$

where:

$$a_n = \frac{1}{\int_a^b rK_1^2(r,\zeta_n)dr} = \frac{\pi^2}{2}\frac{\zeta_n^2\{J_0(\zeta_n b)\}^2}{\{J_0(\zeta_n a)\}^2 - \{J_0(\zeta_n b)\}^2} \quad (20a)$$

$$b_m = \frac{1}{\int_a^b rK_2^2(r,\xi_m)dr} = \frac{\pi^2\xi_m^2 e_2^2}{2\{(h_2^2+\xi_m^2[1-\left(\frac{1}{\xi_m b}\right)^2])e_1^2 - (h_1^2+\xi_m^2[1-\left(\frac{1}{\xi_m a}\right)^2])e_2^2\}} \quad (20b)$$

in which

$$e_1 = \xi_m J_1'(\xi_m a) + h_1 J_1(\xi_m a) \quad (21a)$$

$$e_2 = \xi_m J_1'(\xi_m b) + h_2 J_1(\xi_m b) \quad (21b)$$

Applying the finite Hankel transform to the Eqs. (12) and (14), yields:

$$\frac{\partial\bar{\theta}_1}{\partial t} + \alpha^*\zeta_n^2\bar{\theta}_1(\zeta_n,t) = \alpha^*\left[\frac{2J_0(\zeta_n a)}{\pi J_0(\zeta_n b)}g(t) - \frac{2}{\pi}f(t)\right] = A_1(t) \quad (22a)$$

$$\frac{\partial^2\bar{u}_1(\xi_m,t)}{\partial t^2} + \left(\frac{\xi_m}{\gamma}\right)\bar{u}_1(\xi_m,t) = \frac{1}{\gamma^2}\left[\frac{2e_1}{\pi e_2}B_2(t) - \frac{2}{\pi}B_1(t)\right] = A_2(t) \quad (22b)$$

Eqs. (22a) and (22b) are non-homogeneous ordinary differential equations, the solution of which can be easily obtained as follows:

$$\bar{\theta}_1(\zeta_n,t) = \int_0^t A_1(\tau)e^{-\alpha^*\zeta_n^2(t-\tau)}d\tau \quad (23a)$$

$$\bar{u}_1(\xi_m,t) = \frac{\gamma}{\xi_m}\int_0^t A_2(\tau)\sin\left(\frac{\xi_m}{\gamma}(t-\tau)\right)d\tau \quad (23b)$$

Using the inversion relations, Eqs. (18a) and (18b), we have:

$$\theta_1(r,t) = \sum_{n=1}^{\infty} a_n K_1(r,\zeta_n)\int_0^t A_1(\tau)e^{-\alpha^*\zeta_n^2(t-\tau)}d\tau \quad (24a)$$

$$u_1(r,t) = \sum_{m=1}^{\infty}\frac{\gamma}{\xi_m}b_m K_2(r,\xi_m)\int_0^t A_2(\tau)\sin\left(\frac{\xi_m}{\gamma}(t-\tau)\right)d\tau \quad (24b)$$

As is seen the first set of the equations were solved. To solve the second set of the equations, $\theta_2(r,t)$ and $u_2(r,t)$ can be considered as the following form [2]:

$$\theta_2(r,t) = Q(t)K_1(r,\zeta_n) \quad (25a)$$

$$u_2(r,t) = S(t)K_2(r,\xi_m) \quad (25b)$$

where $Q(t)$ and $S(t)$ are unknown functions of time. It should be emphasized that the above forms for $\theta_2(r,t)$ and $u_2(r,t)$ satisfy the related boundary conditions. Substituting Eqs. (19a), (19b), (25a) and (25b) into (13a) and (15a) yields:

$$(\dot{Q} + \alpha^*\zeta_n^2 Q)K_1(r,\zeta_n) = -\frac{E\alpha T_0}{\rho c(1-2v)}(b_m\dot{\bar{u}}_1 + \dot{S})\left(\frac{\partial K_2(r,\xi_m)}{\partial r} + \frac{K_2(r,\xi_m)}{r}\right) \quad (26a)$$

$$\left(\ddot{S} + \left(\frac{\xi_m}{\gamma}\right)^2 S\right)K_2(r,\xi_m) = -\frac{\beta}{\gamma^2}(a_n\bar{\theta}_1 + Q)\frac{\partial K_1(r,\zeta_n)}{\partial r} \quad (26b)$$

Using the orthogonality of the Bessel functions, the following equations can be obtained [24]:

$$\int_a^b rK_1(r,\zeta_n)K_1(r,\zeta_p)dr = N_n\delta_{np} \quad (27a)$$

$$\int_a^b rK_2(r,\xi_m)K_2(r,\xi_p)dr = M_m\delta_{mp} \quad (27b)$$

where δ is the Kronecker delta and:

$$N_n = \frac{\pi^2}{2}\frac{\zeta_n^2\{J_0(\zeta_n b)\}^2}{\{J_0(\zeta_n a)\}^2 - \{J_0(\zeta_n b)\}^2} \quad (28a)$$

$$M_m = \frac{1}{\xi_m^2}\left\{ b^2 \frac{dK_2}{dr}\Big|_{r=b}^2 - a^2 \frac{dK_2}{dr}\Big|_{r=a}^2 + (\xi_m^2 - 1)[b^2K_2^2(b) - a^2K_2^2(a)] \right\} \tag{28b}$$

Multiplying Eq. (26a) by $rK_1(r,\zeta_n)$ and Eq. (26b) by $rK_2(r,\xi_m)$, integrating between a and b, and then using the orthogonality relations result in:

$$\dot{Q} + \alpha^*\zeta_n^2 Q = \left\{ -\frac{E\alpha T_0 \displaystyle\int_a^b rK_1(r,\zeta_n)\left(\frac{\partial K_2(r,\xi_m)}{\partial r} + \frac{K_2(r,\xi_m)}{r}\right)dr}{\rho c(1-2v)N_n} \right\}(b_m\dot{\bar{u}}_1 + \dot{S}) \tag{29a}$$

$$\ddot{S} + \left(\frac{\xi_m}{\gamma}\right)^2 S = \left\{ -\frac{\beta \displaystyle\int_a^b rK_2(r,\xi_m)\frac{\partial K_1(r,\zeta_n)}{\partial r}dr}{\gamma^2 M_m} \right\}(a_n\bar{\theta}_1 + Q) \tag{29b}$$

To simplify the above equations we introduce the following parameters:

$$U_1 = \left\{ -\frac{E\alpha T_0 \displaystyle\int_a^b rK_1(r,\zeta_n)\left(\frac{\partial K_2(r,\xi_m)}{\partial r} + \frac{K_2(r,\xi_m)}{r}\right)dr}{\rho c(1-2v)N_n} \right\} \tag{30a}$$

$$U_2 = \left\{ -\frac{\beta \displaystyle\int_a^b rK_2(r,\xi_m)\frac{\partial K_1(r,\zeta_n)}{\partial r}dr}{\gamma^2 M_m} \right\} \tag{30b}$$

Now Eqs. (29a) and (29b) can be written in the simplified form:

$$\dot{Q} + \alpha^*\zeta_n^2 Q = U_1(b_m\dot{\bar{u}}_1 + \dot{S}) \tag{31a}$$

$$\ddot{S} + \left(\frac{\xi_m}{\gamma}\right)^2 S = U_2(a_n\bar{\theta}_2 + Q) \tag{31b}$$

The proper form of the initial conditions can be obtained by substituting Eq. (13d) into (25a):

$$Q(0)K_1(r,\zeta_n) = F_1(r) \tag{32}$$

Using the orthogonality relation (27a) leads to:

$$Q(0) = \frac{\int_a^b rK_1(r,\zeta_n)F_1(r)dr}{N_n} \tag{33}$$

The initial conditions for $S(t)$ can be acquired in an identical procedure:

$$S(0) = \frac{\displaystyle\int_b^a rK_2(r,\xi_m)F_2(r)dr}{M_m} \tag{34a}$$

$$\dot{S}(0) = \frac{\int_a^b rK_2(r,\xi_m)F_3(r)dr}{M_m} \tag{34b}$$

It can be that Eqs. (31a) and (31b) are coupled. These coupled equations can be uncoupled by some mathematical operations. By differentiating Eqs. (31a) and (31b) with respect to time we have:

$$\dddot{Q} + \alpha^*\zeta_n^2\ddot{Q} = U_1(b_m\dddot{\bar{u}}_1 + \dddot{S}) \tag{35a}$$

$$\dddot{S} + \left(\frac{\xi_m}{\gamma}\right)^2 \dot{S} = U_2(a_n\dot{\bar{\theta}}_1 + \dot{Q}) \tag{35b}$$

Substituting $\dot{Q}$ from Eq. (31a) in the Eq. (35b) leads to:

$$\dddot{S} + \left(\frac{\xi_m}{\gamma}\right)^2 \dot{S} = U_2[a_n\dot{\bar{\theta}}_1 + U_1(b_m\ddot{\bar{u}}_1 + \dot{S}) - \alpha^*\zeta_n^2 Q] \tag{36}$$

Now by substituting Q from Eq. (31b) into Eq. (36) we have:

$$\dddot{S} + \left(\frac{\xi_m}{\gamma}\right)^2 \dot{S} = U_2\left[a_n\dot{\bar{\theta}}_1 + U_1(b_m\ddot{\bar{u}}_1 + \dot{S}) - \alpha^*\zeta_n^2\left(\frac{1}{U_2}(\ddot{S} + \left(\frac{\xi_m}{\gamma}\right)^2 S) - a_n\bar{\theta}_1\right)\right] \tag{37}$$

As is seen Eq. (37) is independent of Q. Substituting $\dddot{S}$ from Eq. (35b) into Eq. (35a) leads to:

$$\dddot{Q} + \alpha^*\zeta_n^2\ddot{Q} = U_1[b_m\ddot{\bar{u}}_1 + U_2(a_n\dot{\bar{\theta}}_1 + \dot{Q}) - \left(\frac{\xi_m}{\gamma}\right)^2 \dot{S}] \tag{38}$$

Now by substituting $\dot{S}$ from Eq. (31a) into Eq. (38) we have:

$$\dddot{Q} + \alpha^*\zeta_n^2\ddot{Q} = U_1\left[b_m\ddot{\bar{u}}_1 + U_2(a_n\dot{\bar{\theta}}_1 + \dot{Q}) - \left(\frac{\xi_m}{\gamma}\right)^2\left(\frac{1}{U_1}(\dot{Q} + \alpha^*\zeta_n^2 Q) - b_m\dot{\bar{u}}_1\right)\right] \tag{39}$$

Now by ordering Eqs. (37) and (39) $Q(t)$ and $S(t)$ can be obtained in the following form:

$$\frac{d^3S}{dt^3}+\alpha^*\zeta_n^2\frac{d^2S}{dt^2}+\left(\left(\frac{\xi_m}{\gamma}\right)^2-U_1U_2\right)\frac{dS}{dt}$$
$$+\alpha^*\zeta_n^2\left(\frac{\xi_m}{\gamma}\right)^2S$$
$$=b_mU_1U_2\dot{\bar{u}}_1+a_nU_2(\dot{\bar{\theta}}_1+\alpha^*\zeta_n^2\bar{\theta}_1) \quad (40a)$$
$$\frac{d^3Q}{dt^3}+\alpha^*\zeta_n^2\frac{d^2Q}{dt^2}+\left(\left(\frac{\xi_m}{\gamma}\right)^2-U_1U_2\right)\frac{dQ}{dt}$$
$$+\alpha^*\zeta_n^2\left(\frac{\xi_m}{\gamma}\right)^2Q$$
$$=b_mU_1\frac{d}{dt}\left(\ddot{\bar{u}}_1+\left(\frac{\xi_m}{\gamma}\right)^2\bar{u}_1\right)+a_nU_1U_2\dot{\bar{\theta}}_1 \quad (40b)$$

Eqs. (40a) and (40b) are ordinary differential equations. Substituting Eqs. (22a) and (22b) into Eqs. (40a) and (40b) results in:

$$\frac{d^3S}{dt^3}+\alpha^*\zeta_n^2\frac{d^2S}{dt^2}+\left[\left(\frac{\xi_m}{\gamma}\right)^2-U_1U_2\right]\frac{dS}{dt}$$
$$+\alpha^*\zeta_n^2\left(\frac{\xi_m}{\gamma}\right)^2S=U_2[b_mU_1\dot{\bar{u}}_1+a_nA_1(t)] \quad (41a)$$
$$\frac{d^3Q}{dt^3}+\alpha^*\zeta_n^2\frac{d^2Q}{dt^2}+\left[\left(\frac{\xi_m}{\gamma}\right)^2-U_1U_2\right]\frac{dQ}{dt}$$
$$+\alpha^*\zeta_n^2\left(\frac{\xi_m}{\gamma}\right)^2Q=U_2[b_m\dot{A}_2(t)+a_nU_2\dot{\bar{\theta}}_1] \quad (41b)$$

$Q(t,\xi_m)$ and $S(t,\zeta_n)$ can be acquired by solving Eqs. (41a) and (41b). The solutions of the Eqs. (41a) and (41b), depend on the mechanical and the thermal boundary conditions, thus $Q(t,\xi_m)$ and $S(t,\xi_n)$ are presented in the numerical examples section. Then, the solutions for both parts of $\theta(r,t)$ and $u(r,t)$ are obtained and the closed-form relations for the temperature distribution and the displacement are:

$$\theta(r,t)=\sum_{n=1}^{\infty}a_n\bar{\theta}_1(t)K_1(r,\zeta_n)$$
$$+\sum_{m=1}^{\infty}\sum_{n=1}^{\infty}Q(t,\xi_m)K_1(r,\zeta_n) \quad (42a)$$
$$u(r,t)=\sum_{m=1}^{\infty}b_m\bar{u}_1(t)K_2(r,\xi_m)$$
$$+\sum_{m=1}^{\infty}\sum_{n=1}^{\infty}S(t,\zeta_n)K_2(r,\xi_m) \quad (42b)$$

4. Numerical Examples

In order to study the response of the cylinder under external loads, two numerical examples are considered. The material properties of Aluminum are employed in the calculations [26]:

$a=1\text{m};\quad b=2\text{m};\quad P=100\text{MPa};\quad v=0.3;\quad \theta_0=100$

$E=70\text{GPa};\quad \rho=2707\text{kg/m}^3;\quad k=204\text{W/mK}$

$\alpha=23E-6\ 1/K;\quad c=903\text{J/kgK};\quad T_0=29\text{K}$

4.1. Pure Mechanical Load

In the case when only a constant mechanical load is applied on the inner surface of the cylinder and the outer surface is traction free, thermal and mechanical boundary conditions of the problem are:

$$\theta(a,t)=0 \quad (43a)$$
$$\theta(b,t)=0 \quad (43b)$$
$$\sigma_{rr}(a,t)=-P \quad (43c)$$
$$\sigma_{rr}(b,t)=0 \quad (43d)$$

Also the thermal and mechanical initial conditions are:

$$\theta(r,0)=0 \quad (44a)$$
$$u(r,0)=0 \quad (44b)$$
$$\dot{u}(r,0)=0 \quad (44c)$$

Thus we have:

$$Q(0)=0 \quad (45a)$$
$$S(0)=0 \quad (45b)$$
$$\dot{S}(0)=0 \quad (45c)$$

Using Eq. (22a) and the thermal boundary conditions, there is:

$$A_1(t)=0 \quad (46a)$$
$$\bar{\theta}_1(\zeta_n,t)=0 \quad (46b)$$

Using the mechanical boundary conditions and Eqs. (9c) and (9d) we have:

$$B_1=-\frac{P(1+v)(1-2v)}{E(1-v)} \quad (47a)$$
$$B_2=0 \quad (47b)$$
$$A_2(t)=\frac{2P(1+v)(1-2v)}{\pi\gamma^2E(1-v)} \quad (47c)$$

Substituting Eq. (46a) into (23b) gives:

$$\bar{u}_1(\xi_m,t)=\frac{2P(1+v)(1-2v)}{\pi\xi_m^2E(1-v)}\left(1-\cos\left(\frac{\xi_m}{\gamma}t\right)\right) \tag{48}$$

Substituting Eqs. (45b) and (47b) into Eqs. (24a) and (24b) gives:

$$\theta_1(r,t)-0 \tag{49a}$$

$$u_1(r,t)=\frac{2P(1+v)(1-2v)}{\pi E(1-v)}\sum_{m=1}^{\infty}\frac{b_m}{\xi_m^2}\left(1-\cos\left(\frac{\xi_m}{\gamma}t\right)\right)K_2(r,\xi_m) \tag{49b}$$

Using Eqs. (41a) and (41b) we have:

$$\frac{d^3S}{dt^3}+\alpha^*\zeta_n^2\frac{d^2S}{dt^2}+\left(\left(\frac{\xi_m}{\gamma}\right)^2-U_1U_2\right)\frac{dS}{dt}+\alpha^*\zeta_n^2\left(\frac{\xi_m}{\gamma}\right)^2S=R\sin\left(\frac{\xi_m}{\gamma}t\right) \tag{50a}$$

where:

$$R=\frac{2b_mU_1U_2P(1+v)(1-2v)}{\pi E(1-v)\xi_m\gamma} \tag{51}$$

Solving Eqs. (49a) and (49b) results in:

$$S(t)=\frac{R\gamma}{\xi_mU_1U_2}\cos\left(\frac{\xi_m}{\gamma}t\right)+\sum_{i=1}^{3}c_ie^{\alpha_it} \tag{52a}$$

$$Q(t)=\frac{1}{U_2}\sum_{i=1}^{3}\left(\alpha_i^2+\left(\frac{\xi_m}{\gamma}\right)^2\right)c_ie^{\alpha_it} \tag{52b}$$

where α_i's are the roots of the following equation:

$$x^3+\alpha^*\zeta_n^2x^2+\left(\left(\frac{\xi_m}{\gamma}\right)^2-U_1U_2\right)x+\alpha^*\zeta_n^2\left(\frac{\xi_m}{\gamma}\right)^2=0 \tag{53}$$

It should be mentioned that $Q(t)$ is obtained by using Eq. (31b). The constants c_i's can be acquired using Eqs. (45a) to (45c).

$$\begin{pmatrix}c_1\\c_2\\c_3\end{pmatrix}=\begin{pmatrix}1&1&1\\\alpha_1&\alpha_2&\alpha_3\\\alpha_1^2+\left(\frac{\xi_m}{\gamma}\right)^2&\alpha_2^2+\left(\frac{\xi_m}{\gamma}\right)^2&\alpha_3^2+\left(\frac{\xi_m}{\gamma}\right)^2\end{pmatrix}\begin{pmatrix}-\frac{R\gamma}{\xi_mU_1U_2}\\0\\0\end{pmatrix} \tag{54}$$

Eq. (53) is a cubic equation and has three roots, one of which is real negative and the two others are complex conjugate with negative real part. Because of the negative power of these exponential terms, they vanish over time passing. Figs. 2 and 3 present the history of dynamic radial and hoop stresses.

As it is seen, dilatation wave which initiated at the inner surface moves forward from the inner surface and after colliding outer surface reflects into the medium in the opposite direction. Due to the traction free boundary condition of the outer surface, the propagated wave becomes reversed after collision by outer surface. As it is observed from figures stress wave magnitude became smaller after reflecting inward the medium.

Indeed, compressive radial stress wave produces tensile hoop stress. But as is seen at the initial moments when the compressive stress wave reaches different radial positions, tangential stress component becomes compressive and then rises progressively with time. This occurs due to the resistance of the nearby points in the medium which exerts to any point.

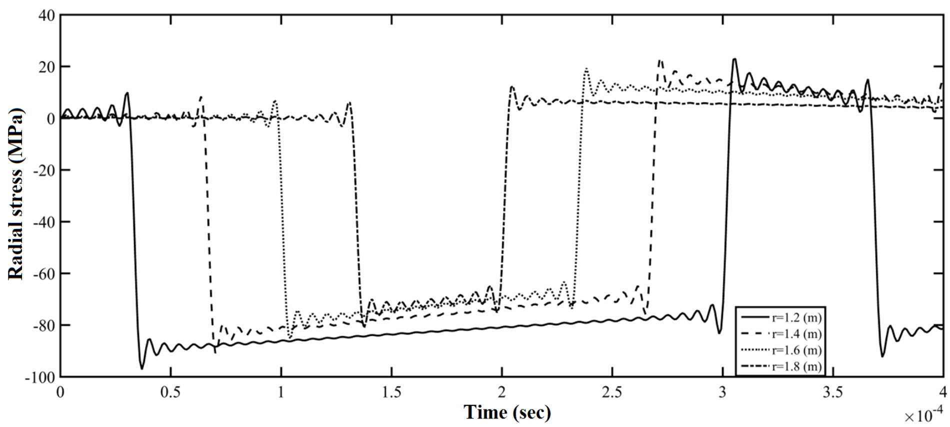

Fig. 2. History of dynamic radial stress for different radial positions (case i).

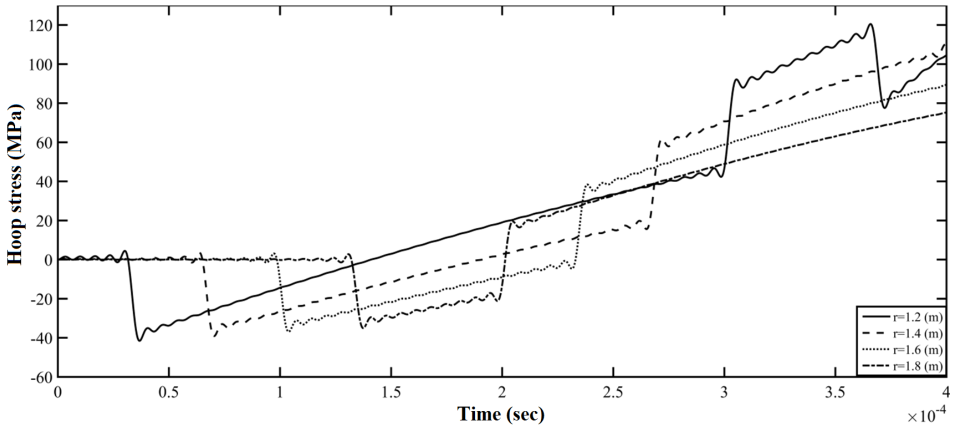

Fig. 3. History of dynamic hoop stress for different radial positions (case i).

As is mentioned, coupled classical theory of thermoelasticity is used to solve the problem. Due to existence of strain rate terms in the energy equation, a change in the amount of strain can produce a temperature change. In this example, there is not any thermal load applied to the cylinder, but because of the coupling term a change in temperature is observed. Fig. 4 shows this temperature difference with respect to the reference temperature.

Figs. 5 and 6 show through-thickness variation of hoop and radial stresses. Velocity of the propagated wave into the cylinder is the reverse square root of the factor of the second derivative of displacement with respect to the time in the equation of motion and can be acquired using the following equation:

$$V_e = \frac{1}{\gamma} = \sqrt{\frac{E(1-v)}{\rho(1+v)(1-2v)}} = 5.9 \times 10^3 (\mathrm{m/s}) \quad (55)$$

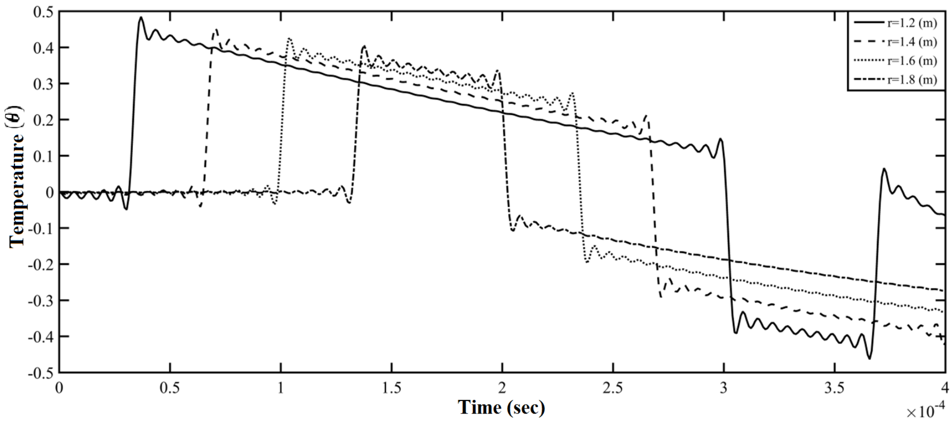

Fig. 4. History of temperature for different radial positions (case i).

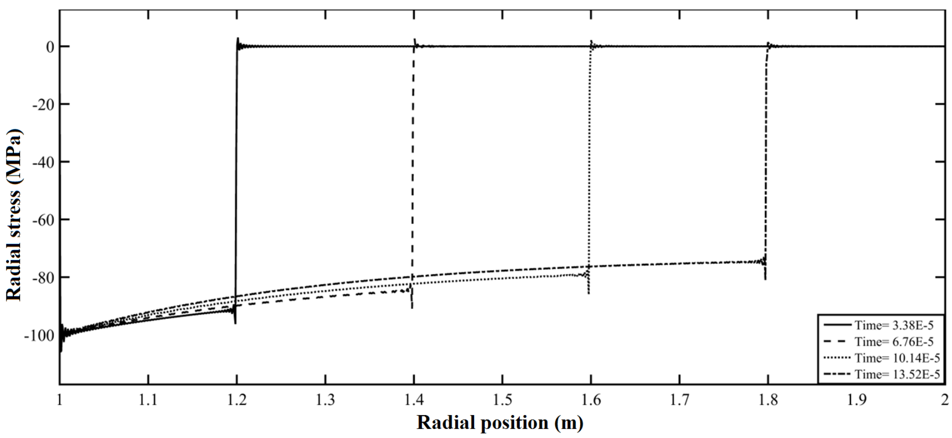

Fig. 5. Through-thickness variation of dynamic radial stress (case i).

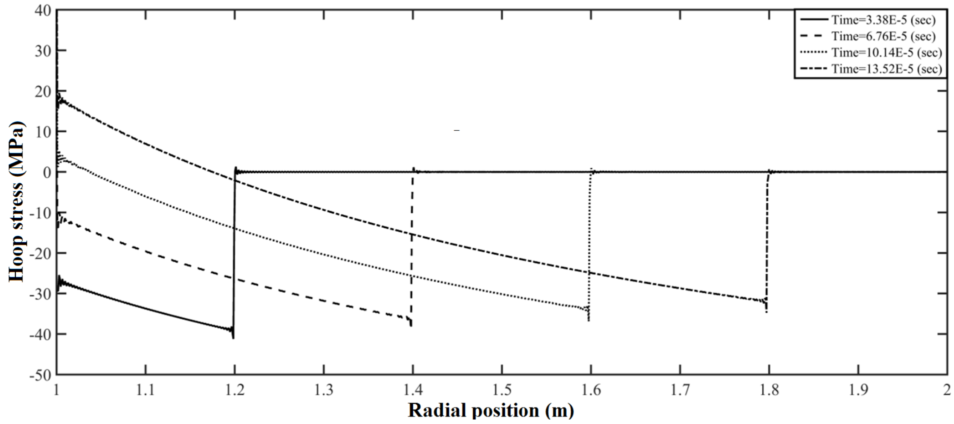

Fig. 6. Through-thickness variation of dynamic hoop stress (case i).

Using Eq. (55) the first time can be calculated when dilatation wave reaches each radial position. For example:

$$t^* = \frac{r-a}{V_e} = \frac{1.2-1}{5.9\times 10^3} = 0.33898\times 10^{-4}(\text{sec}) \quad (56)$$

It is seen from the Figs. 5 and 6 that at the same time as computed in Eq. (56), the stress wave has reached the radial position $r = 1.2$.

As is mentioned due to resistance exerted to any point by medium, tangential component becomes compressive at the initial moments and then proceeds from negative to positive. This reality is obviously shown in the Fig. 6.

4.2. Pure Thermal Load

In this case a constant temperature is applied on the inner surface of the cylinder. So the boundary conditions of the problem are:

$$\theta(a,t) = \theta_0 \quad (57a)$$
$$\theta(b,t) = 0 \quad (57b)$$
$$\sigma_{rr}(a,t) = 0 \quad (57c)$$
$$\sigma_{rr}(b,t) = 0 \quad (57d)$$

The thermal and mechanical initial conditions are:

$$\theta(r,0) = 0 \quad (58a)$$
$$u(r,0) = 0 \quad (58b)$$
$$\dot{u}(r,0) = 0 \quad (58c)$$

Thus we have:

$$Q(0) = 0 \quad (59a)$$
$$S(0) = 0 \quad (59b)$$
$$\dot{S}(0) = 0 \quad (59c)$$

Using the thermal boundary conditions, Eqs. (57a) and (57b), and Eqs. (22a) and (22b) together with Eqs. (9c) and (9d), we have:

$$A_1(t) = -\frac{2\alpha^*\theta_0}{\pi} \quad (60a)$$

$$A_2(t) = -\frac{2\alpha\theta_0(1+v)}{\pi\gamma^2(1-v)} \quad (60b)$$

Using Eqs. (23a) and (23b), leads to:

$$\bar{\theta}_1(\zeta_n,t) = -\frac{2\theta_0}{\pi\zeta_n^2}(1-e^{-\alpha^*\zeta_n^2 t}) \quad (61a)$$

$$\bar{u}_1(\xi_m,t) = -\frac{2\alpha\theta_0(1+v)}{\pi\xi_m^2(1-v)}\left(1-\cos\left(\frac{\xi_m}{\gamma}t\right)\right) \quad (61b)$$

Substituting Eqs. (60a) and (60b) into Eqs. (24a) and (24b), leads to:

$$\theta_1(r,t) = -\frac{2\theta_0}{\pi}\sum_{n=1}^{\infty}\frac{a_n}{\zeta_n^2}(1-e^{-\alpha^*\zeta_n^2 t})K_1(r,\zeta_n) \quad (62a)$$

$$u_1(r,t) = -\frac{2\alpha\theta_0(1+v)}{\pi(1-v)}\sum_{m=1}^{\infty}\frac{b_m}{\xi_m^2}\Bigg(1 - \cos\left(\frac{\xi_m}{\gamma}t\right)\Bigg)K_2(r,\xi_m) \quad (62b)$$

Eqs. (41a) and (41b) then can be written as:

$$\frac{d^3S}{dt^3} + \alpha^*\zeta_n^2\frac{d^2S}{dt^2} + \left((\frac{\xi_m}{\gamma})^2 - U_1U_2\right)\frac{dS}{dt} + \alpha^*\zeta_n^2\left(\frac{\xi_m}{\gamma}\right)^2 S = -U_2\left(b_mU_1\frac{2\alpha\theta_0(1+v)}{\pi\xi_m(1-v)\gamma}\sin\left(\frac{\xi_m}{\gamma}t\right) + a_n\frac{2\alpha^*\theta_0}{\pi}\right) \quad (63a)$$

$$\frac{d^3Q}{dt^3} + \alpha^*\zeta_n^2\frac{d^2Q}{dt^2} + \left((\frac{\xi_m}{\gamma})^2 - U_1U_2\right)\frac{dQ}{dt} + \alpha^*\zeta_n^2\left(\frac{\xi_m}{\gamma}\right)^2 Q = -U_1\left(a_nU_2\frac{2\theta_0\alpha^*}{\pi}e^{-\alpha^*\zeta_n^2 t}\right) \quad (63b)$$

Solving equations (63a) and (63b), there is:

$$S(t) = -\frac{2a_n\theta_0 U_2}{\pi\zeta_n^2\left(\frac{\xi_m}{\gamma}\right)^2} - \frac{2b_m\alpha(1+v)\theta_0}{\pi\xi_m^2(1-v)}\cos\left(\frac{\xi_m}{\gamma}t\right) + \sum_{i=1}^{3} c_i e^{\alpha_i t} \tag{64a}$$

$$Q(t) = -\frac{2a_n\theta_0}{\pi\zeta_n^2}e^{-\alpha^*\zeta_n^2 t} + \frac{1}{U_2}\sum_{i=1}^{3}\left(\alpha_i^2 + \left(\frac{\xi_m}{\gamma}\right)^2\right)c_i e^{\alpha_i t} \tag{64b}$$

where α_i's are the roots of Eq. (53) and the constants c_i can be acquired using Eqs. (59a) to (59c):

The Stress components are shown in Figs. 7 and 8. Applying thermal load on the inner surface at the earlier moments causes a thermal shock which is observed in figures. Similar to the mechanical load, dilatation wave which is produced at the inner surface moves forward from the inner surface and after colliding outer surface reflects into the medium in the opposite direction.

The temperature field has the exponential distribution with time, and it takes time the thermal load effect reaches any radial position and makes a change in stress components. Contrariwise the pure mechanical load case, in the pure thermal load radial stress wave is tensile and produces compressive hoop stress. When the tensile wave reaches a specific radial position, the tangential stress component immediately becomes tensile owing to the resistance of the nearby points in the medium and decays gradually with time.

$$\begin{pmatrix} c_1 \\ c_2 \\ c_3 \end{pmatrix} = \frac{2\theta_0}{\pi}\begin{pmatrix} 1 & 1 & 1 \\ \alpha_1 & \alpha_2 & \alpha_3 \\ \alpha_1^2 + \left(\frac{\xi_m}{\gamma}\right)^2 & \alpha_2^2 + \left(\frac{\xi_m}{\gamma}\right)^2 & \alpha_3^2 + \left(\frac{\xi_m}{\gamma}\right)^2 \end{pmatrix}^{-1}\begin{pmatrix} \frac{a_n U_2}{\zeta_n^2\left(\frac{\xi_m}{\gamma}\right)^2} + \frac{b_m\alpha(1+v)}{\xi_m^2(1-v)} \\ 0 \\ \frac{a_n U_2}{\zeta_n^2} \end{pmatrix} \tag{65}$$

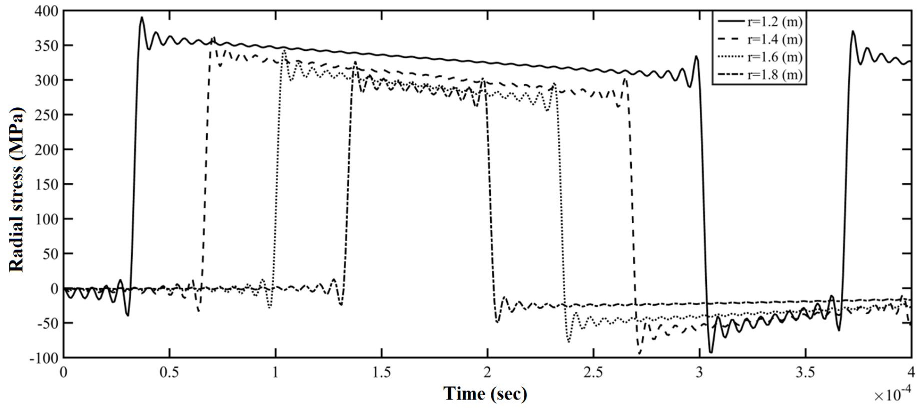

Fig. 7. History of dynamic radial stress for different radial positions (case ii).

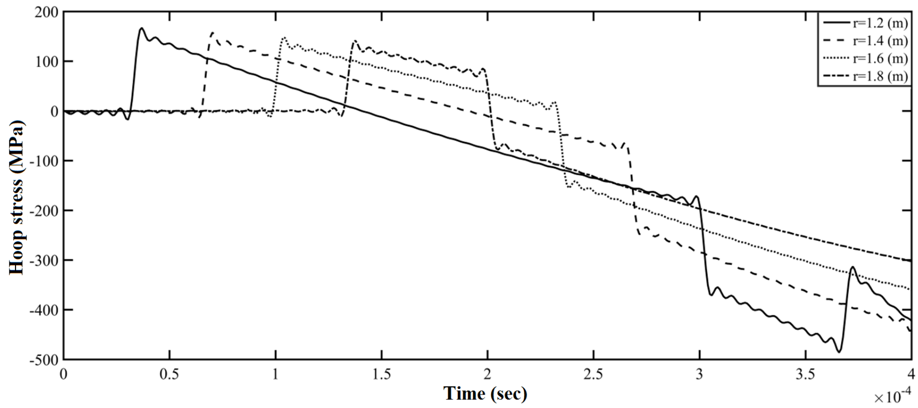

Fig. 8. History of dynamic hoop stress for different radial positions (case ii).

Fig. 9 shows the temperature difference with respect to the reference temperature. Due to plotting the figure in short period of time, the coupling effect is main part of temperature history.

Figs. 10 and 11 shows the through-thickness variation of radial and hoop stress components.

As is mentioned due to resistance of nearby points, tangential component becomes tensile at the initial moments and then proceeds from positive to negative. This reality is obviously shown in the Fig. 11.

5. Validation

The present work is validated in a special case with the problem of isotropic cylinder subjected to uniform temperature throughout the cylinder. In the mentioned problem, the energy equation has not been solved and a constant temperature is assumed for all radial sections of the cylinder and therefore there is no temperature gradient. The history of non-dimensional stress components are plotted in Figs. 12 and 13. The corresponding results of Ding et al. [9] are on the same figures.

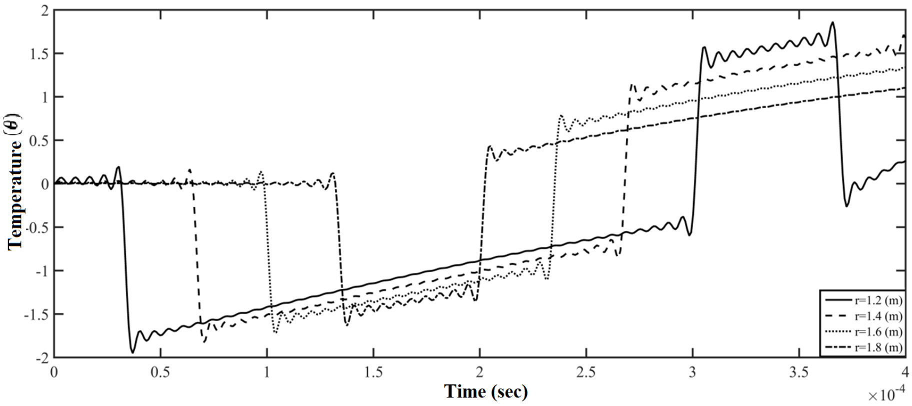

Fig. 9. History of temperature for different radial positions (case ii).

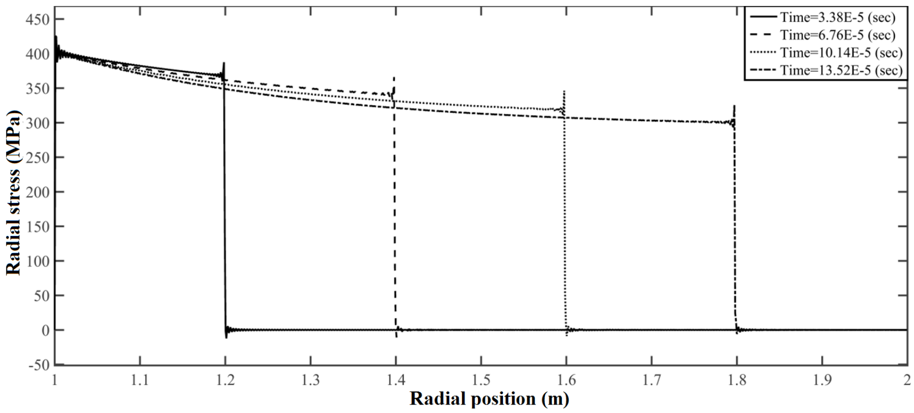

Fig. 10. Through-thickness variation of dynamic radial stress (case ii).

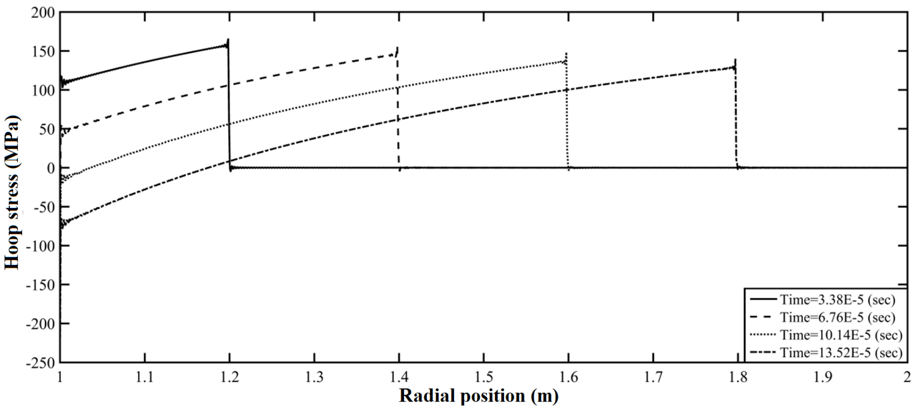

Fig. 11. Through-thickness variation of dynamic hoop stress (case ii).

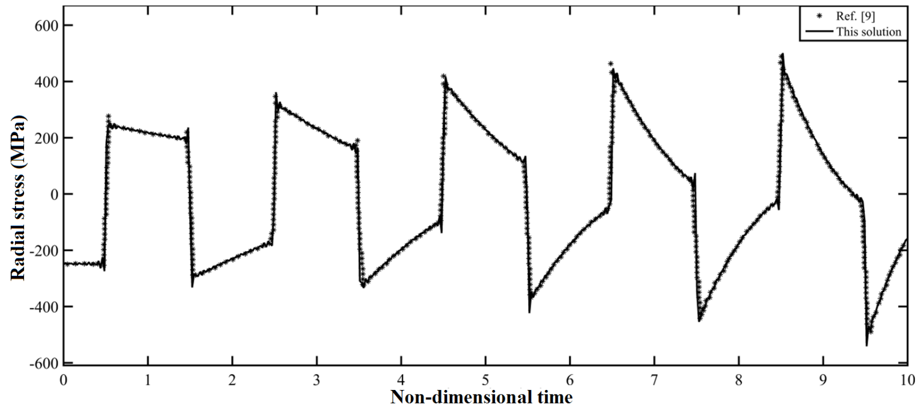

Fig. 12. Variation of radial stress for $r = \dfrac{a+b}{2}$.

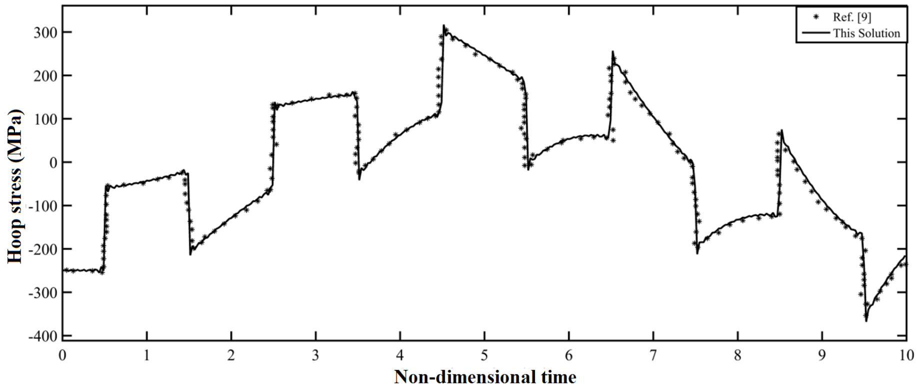

Fig. 13. Variation of hoop stress for $r = \dfrac{a+b}{2}$.

It is observed that the results of the current work are in good agreement with the results of Ding et al. [9] and the validation of the solution is verified. The non-dimensional time relation used in the figures is defined as follows:

$$\bar{t} = \frac{V_e t}{a} \tag{66}$$

Due to applying thermo-mechanical boundary conditions in the inner and the outer surfaces of the cylinder, there are two thermo-elastic waves. The one moves outward from the inner surface and the other propagates inward the cylinder from the outer surface.

6. Conclusions

The fully coupled dynamic thermoelasticity problem in a thick hollow cylinder is solved analytically and closed-form relations are presented for temperature distribution and stress components. The effect of the thermo-mechanical coupling and the propagation of stress waves into the medium for two different cases are illustrated in the figures and the following conclusions were drawn:

1. Considering thermo-mechanical coupling term in the heat conduction equation leads to producing induced temperature gradient.
2. Produced heat due to thermo-mechanical coupling term in the heat conduction equation depends on strain rate, the mechanical and thermal properties of the material.
3. Induced temperature in adherence to elastic and thermoelastic waves has the wave nature and exactly at the moment that compressive or tensile stress wave reaches any radial position increases or decreases.
4. As it was expected traction free boundary condition reverses the propagated stress wave and compressive stress wave reflects into the medium as tensile and vice-versa.
5. Regarding the validation section figures, thermoelastic stress wave propagates into the medium even in the absence of temperature gradient. In addition, applying non-zero boundary condition on the outer surface of the cylinder leads to another thermo-elastic wave initiating from this surface.

References

[1] A.R. Shahani, S. Momeni Bashusqeh, Analytical solution of the thermoelasticity problem in a pres-

surized thick-walled sphere subjected to transient thermal loading, Math. Mech. Solids, 19(2) (2014) 135-151.

[2] A.R. Shahani, S. Momeni Bashusqeh, Analytical solution of the coupled thermo-elasticity problem in a pressurized sphere, J. Therm. Stresses, 36(12) (2013) 1283-1307.

[3] A.R. Shahani, S.M. Nabavi, Analytical solution of the quasi-static thermoelasticity problem in a pressurized thick-walled cylinder subjected to transient thermal loading, Appl. Math. Model., 31(9) (2007) 1807-1818.

[4] Y. Yun, I.Y. Jang, L. Tang, Thermal stress distribution in thick wall cylinder under thermal shock, J. Press. Vessel Technol., 131(2) (2009) 021212.

[5] M. Raoofian Naeeni, M. Eskandari-Ghadi, A.R. Ardalan, M. Rahimian, Y. Hayati, Analytical Solution of Coupled Thermoelastic Axisymmetric Transient Waves in a Transversely Isotropic Half-Space, J. Appl. Mech., 80(2) (2013) 024502.

[6] W. Liang, S. Huang, W.S. Tan, Y.Z. Wang, Asymptotic approach to transient thermal shock problem with variable material properties, Mech. Adv. Mater. Struct., 26(4) (2019) 350-358.

[7] X. Wang, Thermal shock in a hollow cylinder caused by rapid arbitrary heating, J. Sound Vib., 183(5) (1995) 899-906.

[8] H. Cho, G.A. Kardomateas, C.S. Valle, Elastodynamic solution for the thermal shock stresses in an orthotropic thick cylindrical shell, J. Appl. Mech., 65(1) (1998) 184-193.

[9] H.J. Ding, H.M. Wang, W.Q. Chen, A solution of a non-homogeneous orthotropic cylindrical shell for axisymmetric plane strain dynamic thermoelastic problems, J. Sound Vib., 263(4) (2003) 815-829.

[10] J. Zhou, Z. Deng, X. Hou, Transient thermal response in thick orthotropic hollow cylinders with finite length: high order shell theory, Acta Mech. Solida Sin., 23(2) (2010) 156-166.

[11] S.S. Vel, Exact thermoelastic analysis of functionally graded anisotropic hollow cylinders with arbitrary material gradation. Mech. Adv. Mater. Struct., 18(1) (2011) 14-31.

[12] M. Marin, On the domain of influence in thermoelasticity of bodies with voids, Arch. Math., 33(4) (1997) 301-308.

[13] A.V. Rychahivskyy, Y.V. Tokovyy, Correct analytical solutions to the thermoelasticity problems in a semi-plane, J. Therm. Stresses, 31(11) (2008) 1125-1145.

[14] A.R. Shahani, H. Sharifi Torki, Analytical solution of the thermoelasticity problem in thick-walled cylinder subjected to transient thermal loading, Modares Mechanical Engineering, 16(10) (2016) 147-154.

[15] A.R. Shahani, H. Sharifi Torki, Determination of the thermal stress wave propagation in orthotropic hollow cylinder based on classical theory of thermoelasticity, Contin. Mech. Thermodyn., 30(3) (2018) 509-527.

[16] J.Q. Tarn, Exact solutions for functionally graded anisotropic cylinders subjected to thermal and mechanical loads, Int. J. Solids Struct., 38(46) (2001) 8189-8206.

[17] C. Itu, C. Itu, A. Ochsner, S. Vlase, M. Marin, Improved rigidity of composite circular plates through radial ribs, Proceedings of the Institution of Mechanical Engineers, Part L: Journal of Materials: Design and Applications. 233(8) (2018) 1585-1593.

[18] P. Lata, I. Kaur, Thermomechanical interactions in transversely isotropic thick circular plate with axisymmetric heat supply, Struct. Eng. Mech., 69(6) (2019) 607-614.

[19] S. Vlase, M. Marin, AOchner, M.L. Scutaru, Motion equation for a flexible one-dimensional element used in the dynamical analysis of a multibody system, Continuum Mech. Thermodyn., 31(1) (2018) 715-724.

[20] K.C. Mishra, J.N. Sharma, P.K. Sharma, Analysis of vibrations in a non-homogeneous thermoelastic thin annular disk under dynamic pressure, Mech. Based Des. Struct. Mach., 45(2) (2017) 207-218.

[21] D.K. Sharma, D. Thakur, V. Walia, N. Sarkar, Free vibration analysis of a nonlocal thermoelastic hollow cylinder with diffusion, J. Therm. Stresses, 43(8) (2020) 981-997.

[22] I.A. Abbas, Analytical solution for a free vibration of a thermoelastic hollow sphere, Mech. Based Des. Struct. Mach., 43(3) (2015) 265-276.

[23] N. Noda, R.B. Hetnarski, Y. Tanigawa, Thermal Stresses, New York: Taylor & Francis, (2003).

[24] I.N. Sneddon, The Use of Integral Transform, New York: Mc-Graw-Hill Book Company, (1972).

[25] G. Cinelli, An extension of the finite hankel transform and applications, Int. J. Eng. Sci., 3(5) (1965) 539-559.

[26] M. Jabbari, H. Dehbani, M.R. Eslami, An exact solution for classic coupled thermoelasticity in cylindrical coordinates, J. Press. Vessel Technol., 133(1) (2011) 051204.